

Investigation of Current, Temperature, and Concentration Distribution of a Solid Oxide Fuel Cell with Mathematical Modelling Approach

S.Mehdi Rezvan¹, Mohammad Ahangari¹, Nagihan Delibaş^{2*}, Soudabeh Bahrami¹, Asgar Moradi¹, Aligholi Niaei^{1,2}

¹Department of Chemical & Petroleum Engineering, University of Tabriz, Tabriz, Iran

²Department of Physics, Faculty of Science, University of Sakarya, 54050 Serdivan, Sakarya, Türkiye

Article History

Received: 21.05.2022

Accepted: 06.09.2022

Published: 05.03.2023

Research Article

Abstract – The usage of environment-friendly energy converter devices is getting more and more attention as a result of environmental crises and regulations. SOFCs are among the highly efficient chemical to electrical energy converters. Thus, their effectiveness is a significant issue to improve. To increase the efficiency of SOFCs, their properties should be investigated. However, it is costly and time-consuming to test all the important characteristics of a solid oxide fuel cell by experimental methods. Computational methods can contribute to evaluate the influence of each parameter on the performance of the fuel cell. In this paper, a 3D mathematical model of a SOFC is presented. The model can describe the fuel cell's temperature, the concentration of material, and current distribution inside the cell. Also, the influence of the flow pattern (co-current and counter-current) on the distribution plots and performance of the solid oxide fuel cell is investigated. The results demonstrate that the distribution of the current, concentration, and temperature is firmly related and wherever the concentration of reactants is higher, the temperature and current increase too. Also, the plots of power density and cell potential versus current were consistent with the results of the literature. Moreover, the comparison between two types of flow patterns shows that there is no significant variation when the type of current changes from counter to co-current. However, the performance of the SOFC is mildly better with a co-current flow pattern.

Keywords – Flow pattern, fuel cell, mathematical modeling, SOFC,

1. Introduction


Fuel cells are one of the most important electrical energy sources since they convert chemical energy to electrical energy directly. The direct conversion of energies decreases the energy losses that occur in conventional conversion of fuel energies to electricity which is through heat (Ferriday & Middleton, 2021; Shaari, et. al., 2021; Singh, et. al., 2021).

Among different types of fuel cells, solid oxide fuel cells attract a lot of attention because of their advantages like being safer than fuel cells with liquid electrolytes and higher efficiency at high temperatures. Not only SOFCs have high-energy efficiency and power density, but also they emit low or zero amounts of pollutants and, because they work at high temperatures (600-1000 °C) they can use various materials as fuel (hydrocarbons, hydrogen or ammonia) (Delibaş et al., 2022; Hussain & Yangping, 2020; Kurahashi et al., 2022; Laosiripojana et al., 2009).

¹  rezvan.amir80@gmail.com

²  m.ahangare95@gmail.com

³  caylak@sakarya.edu.tr

⁴  sudabebahrami68@yahoo.com

⁵  asgharmoradi1374@gmail.com

⁶  ali.niaei@gmail.com

* Corresponding Author

SOFCs have different operating parts. However, the most significant parts are two electrodes and the electrolyte between them. Anode and cathode electrodes should be porous, ion conductor, electron conductor, thermally compatible with the electrolyte and stable at high temperatures. The electrolyte which locates between two electrodes should possess some special properties, like being dense, ion conductor, thermally compatible with electrodes, stable in both reduction and oxidation environments and a weak electron conductor, or not being electron conductor at all (Ahmad et al., 2021; Burnwal, et. al., 2016). In the cathode, the oxygen reduction reaction (ORR) happens, as (1.1), and then the oxygen transfers to the anode through the electrolyte and in the anode, where the hydrogen turn to the proton, oxygen ions and protons react and turn to water, as (2.1) (Aydın, Matsumoto, & Shiratori, 2021; Kurahashi, Murase, & Santander, 2022; Stambouli & Traversa, 2002).



In this reaction, electrons are released and move to the cathode and in this way electricity required for transport or electronic devices can be produced. Figure 1 (Shu et al., 2019). demonstrates the operation of SOFC with H_2 as fuel.

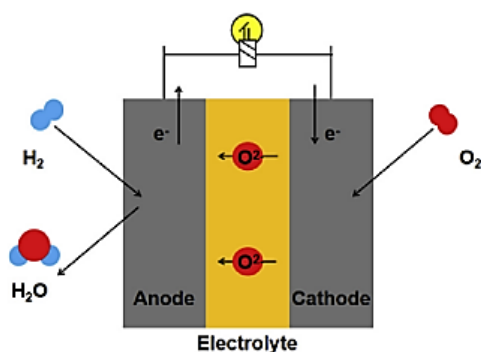


Figure 1. Schematic diagram of operation of a SOFC (Shu et al., 2019)

Numerous parameters such as geometrical properties, type of fuel, electrode and electrolyte material, type of flow etc. affect the performance and efficiency of SOFCs. Since investigating all of these parameters in labs and through experimental work is costly and can be a waste of time, researchers suggest computational work to avoid these problems and study the influence of each parameter in shorter time with much lower cost. In other words, numerical study can contribute to investigating the influence of different geometrical characteristics of the cell without producing different cells, which are expensive, measuring the effect of different materials like anode, cathode and electrolyte, which is difficult to test, studying the distribution of materials' concentration, temperature and charge inside each part of the cell which is impossible to be done experimentally (Abdalla et al., 2018).

There are numerous studies regarding mathematical modeling and simulation of SOFCs and researchers have utilized different approaches to model SOFCs and investigate their properties. For instance, COMSOL Multiphysics software is one of the practical and user-friendly software that can be utilized for studying various aspects of the problem since it contains numerous physics related to mass, heat and charge transform. It also provides various kinds of modeling and simulation such 1D, 2D, and 3D. Moreover, the results can be shown as plots or in the geometry of the problem itself, which is very important in understanding the performance of the fuel cells (Kakac et al., 2007).

Ranasinghe et al, studied the modeling of a single solid oxide fuel cell with COMSOL and reported that the performance of the fuel cell is better when the gas flow pattern is radial rather than a counter flow pattern (Ranasinghe & Middleton, 2017).

Yakabe et al, investigated a three-dimensional mathematical modeling of a planar SOFC and studied the temperature, potential, and chemical species distribution and calculated current density with a finite volume method (Yakabe et al., 2001).

Li et al proposed a quasi 2D model of a tubular SOFC and studied the performance of the cell under the operating condition. The results demonstrated that the quasi approximations used in the model can work well (Li & Suzuki, 2004).

Andersson et al, investigated the material structure grading of a solid oxide fuel cell in the direction normal to the electrode/electrolyte interface and claimed that grading the electron tortuosity and the pore tortuosity in the direction normal to the electrode/electrolyte interface increases performance, but grading the porosity has negative effect on the performance (Xia et al., 2002).

Parametric and transient analysis of non-isothermal, planar Solid oxide fuel cells with COMSOL modeling was studied by Tseronis et al, and they reported the temperature, species composition, electronic and ionic voltage, and current density distributions in a single cell. They also studied the dynamics of SOFC as a result of altering the operation condition of the fuel cell (Tseronis et al., 2012).

The results of the study of Akkaya, which worked on a turbular solid oxide fuel cell, showed that operating conditions play an important role in order to have a fuel cell with optimal performance. Therefore, the change in the operating conditions directly affects the performance of the solid oxide fuel cell. In addition, concentration of polarization is also an important key in limiting the current density (Akkaya, 2007).

Ebrahimi et al, found the optimized fuel cell operation condition using a 3D modeling of transport phenomena in a planar anode-supported solid oxide fuel cell (Chiu et al., 2012).

In this work, we focused on the 3D modeling of a planar solid oxide fuel cell with Yttria-Stabilized Zirconia (YSZ) as electrolyte of the cell, NiO/YSZ (wt.%: 60/40) and $\text{La}_{0.6}\text{Sr}_{0.4}\text{MnO}_3$ were used as anode and cathode materials, respectively. Oxygen flows into the cathode electrode and hydrogen is considered as the fuel of the cell in the anode electrode. The distribution of the concentration of O_2 and H_2 , charge, temperature distribution inside the cell and current distribution are investigated and the plots of the potential and power densities versus current density are demonstrated. All of this data is obtained for both conditions of the current. In other words, the study was done for both co-current and counter current flow pattern inside the fuel cell when the inlet temperature of currents was considered to be 1000 °C (Tseronis et al., 2012, Ranasinghe & Middleton, 2017).

2. SOFC Modeling

First we draw a cross section of our desired SOFC in 2D, it is turned into a three-dimensional model. (Figure 2, Figure 3)

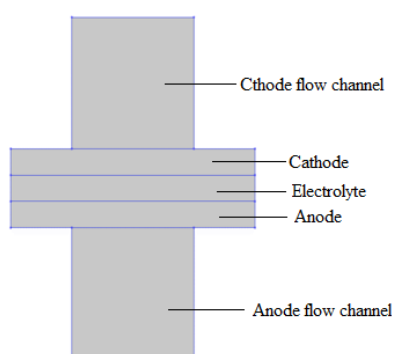


Figure 2. 2D model of SOFC

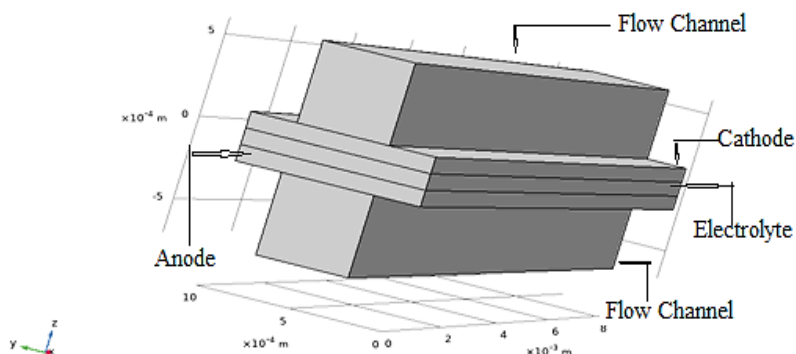


Figure 3. 3D model of SOFC

The physics used for this model are as follows:

- Secondary Current Distribution
- Equations of gas diffusion in porous media and flow channels
- Transport of Concentrated Species
- Heat Transfer in Solids and Fluids

The values of input electrochemical and geometric parameters used in SOFC modeling are given in Table 1 (Ilbas & Kumuk, 2019; Ranasinghe & Middleton, 2017; Suzuki, Shikazono, Fukagata, & Kasagi, 2008; Wang, Yang, Zhang, & Xia, 2007). The OCV in this study is very close to the Nernst value (1.097 V) (Caliandro, Diethelm, & Nakajo, 2015).

Table 1
Parameters used in SOFC model

Value	Parameter	Value	Parameter
Atmospheric pressure	1 [atm]	Air mixture thermal conductivity	0.58 [W.m ⁻¹ .K ⁻¹]
Temperature	800-1000 [C]	Inlet weight fraction H ₂ at anode	0.4
Viscosity, air	3e ⁻⁵ [Pa.s]	Inlet weight fraction O ₂ at cathode	0.15
Pressure drop, anode	2 [Pa]	Electrolyte conductivity	5 [S.m ⁻¹]
Pressure drop, cathode	6 [Pa]	Molecular weight H ₂	2 [g.mol ⁻¹]
Exchange current density, anode	0.1 [A.m ⁻²]	Molecular weight O ₂	32 [g.mol ⁻¹]
Exchange current density, cathode	0.01 [A.m ⁻²]	Molecular weight N ₂	28 [g.mol ⁻¹]
Active specific surface area, cathode	1e ⁹ [1.m ⁻¹]	Molecular weight H ₂ O	18 [g.mol ⁻¹]
Initial cell polarization	0.05 [V]	Gas flow channel width	
Anode permeability	1e ⁻¹⁰ [m ²]	Rib width	0.5e ⁻³ [m]
Cathode permeability	1e ⁻¹⁰ [m ²]	Gas diffusion electrode thickness	0.5e ⁻³ [m]
Equilibrium voltage, anode	0 [V]	Electrolyte thickness	1e ⁻⁴ [m]
Equilibrium voltage, cathode	1 [V]	Gas flow channel height	1e ⁻⁴ [m]
Ionic effective conductivity, anode	1 [S.m ⁻¹]	Flow channel length	0.5e ⁻³ [m]
Electrical effective conductivity, anode	1000 [S.m ⁻¹]	Gas flow channel width	10e ⁻³ [m]
Fuel mixture thermal conductivity	0.32 [W.m ⁻¹ .K ⁻¹]	Flow channel length	0.5e ⁻³ [m]

2.1. Secondary Current Distribution

By using this physics, the relationship between charge transfer and over potential can be described using the Butler-Volmer and Tafel equations. Since the current from the solid oxide fuel cell is generated during an electrochemical reaction at the electrode/electrolyte material interface, it is necessary to correctly determine the kinetics of this reaction. The Butler-Volmer equation is an important equation in electrochemistry that can be used to balance the charge between current and overvoltage η . The general form of the Butler-Volmer equation, which was also used in this simulation, is as follows (Ilbas & Kumuk, 2019):

$$i = i_0 \left[\left(\frac{C_o}{C_o^*} \right) \exp\left(\frac{\alpha_a F \eta}{RT}\right) - \left(\frac{C_r}{C_r^*} \right) \exp\left(-\frac{\alpha_c F \eta}{RT}\right) \right] \quad (2.1)$$

where i is the electrode current density, i_0 exchange current density, C_o and C_r refer to the concentration of the species to be oxidized and to be reduced, respectively, F is the Faraday's constant, R is the gas constant, T is the temperature, η is the overvoltage, α_c cathodic charge transfer coefficient and α_a anodic charge transfer coefficient. Since the current distribution is dependent on the electrochemical reaction and any reaction is also dependent on the concentration of the species participating in the reaction, therefore, the use of this form of the Butler-Volmer equation, which shows the dependence of the current distribution to the concentration of oxidant and reducer species, will be required.

The overvoltage is defined by (Ranasinghe & Middleton, 2017; Yaoxuan, Cheng, & Kening, 2021):

$$\eta = \phi_{\text{electronic}} - \phi_{\text{ionic}} - \Delta\phi_{\text{eq}} \quad (2.2)$$

where $\Delta\phi_{\text{eq}}$ is the equilibrium potential difference.

The cathode and anode charge transfer kinetics is given by (2.3) and (2.4) equations respectively:

$$i = i_{0,c} \left[\exp\left(\frac{3.5F\eta}{RT}\right) - x_{O_2} \left(\frac{C_t}{C_{O_2,\text{ref}}} \right) \exp\left(-\frac{0.5F\eta}{RT}\right) \right] \quad (2.3)$$

$$i_{a,ct} = i_{0,a} \left[\left(\frac{C_{H_2}}{C_{H_2,\text{ref}}} \right) \exp\left(\frac{0.5F\eta}{RT}\right) - \left(\frac{C_{H_2O}}{C_{H_2O,\text{ref}}} \right) \exp\left(-\frac{1.5F\eta}{RT}\right) \right] \quad (2.4)$$

where $i_{0,c}$ and $i_{0,a}$ refer to the cathode exchange current density and anode exchange current density respectively, x_{O_2} is the molar fraction of O_2 , ch_2 is the molar concentration of H_2 , ch_{2O} is the molar concentration of H_2O , ct is the total concentration of species, $ch_{2,\text{ref}}$ and $ch_{2O,\text{ref}}$ is the reference molar concentrations.

We used the anode inlet voltage as a fixed reference voltage which is equal to zero. Also the cathode inlet voltage (V_{cell}) is given by:

$$V_{\text{cell}} = \Delta\phi_{\text{eq,a}} - \Delta\phi_{\text{eq,c}} - V_{\text{pol}} \quad (2.5)$$

In this model, $\Delta\phi_{\text{eq,a}} = 0$ V, $\Delta\phi_{\text{eq,c}} = 1$ V and 0.05 V $< V_{\text{pol}} < 0.8$ V was considered. In addition to the above boundary conditions, the initial condition $\phi_{\text{electronic}} = 0$ and $\phi_{\text{ionic}} = 0$ was considered for the anode and electrolyte, while according to the selected boundary conditions, the initial condition $\phi_{\text{electronic}} = V_{\text{cell}}$ and $\phi_{\text{ionic}} = 0$ was applied to the cathode. We have applied the insulating boundary conditions for all the external boundaries for the ionic charge balance equations of the model.

2.2. Equations of gas diffusion in porous media and flow channel

In the solid oxide fuel cell, there are two fluids, one is the air fluid, which reaches the surface of the cathode material through the channel on the cathode side, so that the oxygen inside it performs the electrochemical reaction of the cathode half-cell. The other fluid is the fuel, which reaches the surface of the anode material through a channel on the anode side. Both air and fuel fluids, when they reach the surface of the porous

electrode material, diffuse and transfer in this porous electrode. Therefore, it is necessary to model fluid transport in both gas flow channel and porous media through appropriate equations

Gas flows in open channels are modelled by using the weakly compressible Navier-Stokes equation as given below (Ilbas & Kumuk, 2019).

$$\rho \left(\frac{\partial \mathbf{u}}{\partial t} + \mathbf{u} \cdot \nabla \mathbf{u} \right) = -\nabla p + \nabla (\mu (\nabla \mathbf{u}) + (\nabla \mathbf{u})^T) - \frac{2}{3} \mu (\nabla \mathbf{u}) \mathbf{I} + \mathbf{F} \quad (2.6)$$

where \mathbf{u} is the fluid velocity, \mathbf{F} is volume force vector, p is the fluid pressure, ρ is the fluid density, \mathbf{I} is identity tensor and μ is the fluid dynamic viscosity.

Also, the Brinkman equations are used for gas diffusion in porous electrodes. This equation is given by (Ranasinghe & Middleton, 2017):

$$\nabla p = -\frac{\mu}{\kappa} \mathbf{v} + \mu_e \nabla^2 (\mathbf{v}) \quad (2.7)$$

where \mathbf{v} is fluid velocity, μ is fluid dynamic viscosity, μ_e is the effective viscosity parameter. At the inlet of the cathode and anode flow channel, the pressure was considered 6 and 4 Pa, respectively. Also, the outlet of the cathode and anode flow channel, the pressure was applied 0 Pa as boundary conditions.

2.3. Transport of Concentrated Species

For each electrode flow compartment (anode and cathode flow channels), the material transport is modelled by the Maxwell-Stefan's diffusion and convection equations. The Maxwell-Stefan diffusion and convection equation given by:

$$\frac{\partial \rho \omega_i}{\partial t} + \nabla \cdot (\mathbf{j}_i + \rho \omega_i \mathbf{u}) = R_i \quad (2.8)$$

where ρ denotes the density, ω_i the mass fraction, \mathbf{j}_i is the molecular flux and R_i is the reaction rate of the i^{th} species, \mathbf{u} is the velocity.

The boundaries at the walls of the gas channels and the electrodes are considered as zero mass flux (insulation condition). We considered the outlet conditions as convective flux. This means that the component transport is perpendicular to the boundary. Furthermore, it is assumed that there is continuity in all the transport compositions. At the inlet of the air and fuel flow channel, the mass fraction of O_2 and H_2 was considered to be 0.15 and 0.4, respectively.

2.4. Heat Transfer in Solids and Fluids

The general equation of heat transfer intended for the model is given below. In this model, we used steady state heat transfer and considered the convection heat transfer only for gas channels. In addition, we ignored radiation heat transfer (Tseronis, Bonis, Kookos, & Theodoropoulos, 2012).

$$\rho \cdot c_p \cdot \mathbf{u} \cdot \nabla T = \nabla \cdot (\mathbf{k} \nabla T) + Q \quad (2.9)$$

Here Q is the heat generation or consumption, \mathbf{k} the effective thermal conductivity, T the temperature and c_p the specific heat capacity. Heat generated by electrochemical suction, ohmic polarization and etc. given by (Mohammad Ebrahimi, 2017; Tseronis et al., 2012):

$$Q = i \cdot \left(\frac{T \cdot \Delta S_r}{n_e \cdot F} + \eta \right) + \sum \frac{i^2}{\sigma} + \sum (r_{\text{ref}} \cdot \Delta H_{\text{ref}}) \quad (2.10)$$

where ΔS_r is entropy change of the reaction, r_{ref} the reforming reaction rates ($\text{mol}/\text{m}^3\text{s}$) and ΔH_{ref} the enthalpy of the reactions.

The heat exchange at the interface between the electrode material and the gas flow (fuel or air) is conductive in the electrode material and convection in the gas flow. Therefore, the following boundary condition can be considered for the interface between the electrode material and the air or fuel flow (Grondin et al., 2013):

$$n \cdot (-k\nabla T) = h \cdot (T_w - T_f) \tag{2.11}$$

where T_w is the channel wall temperature and T_f is the fluid temperature. h is the heat transfer coefficient in gas flow channels is calculated using the Nusselt number ($Nu \approx 3.09$) (Grondin et al., 2013) according to the following equation:

$$h = \frac{Nu \cdot k_{gas}}{D_h} \tag{2.12}$$

D_h is hydraulic diameter for the channel is also given by:

$$D_h = \frac{2 W_{CH} H_{CH}}{W_{CH} + H_{CH}} \tag{2.13}$$

Where W_{CH} and H_{CH} , the length and height of gas channels are respectively. After choosing the suitable physics and boundary conditions, the mesh of the fuel cell is adjusted (Figure 4) and the results of the model obtained by computing and solving the model with FEM. As it is shown in Figure 4 Mesh is finer in electrodes and electrolyte in comparison with flow channels.

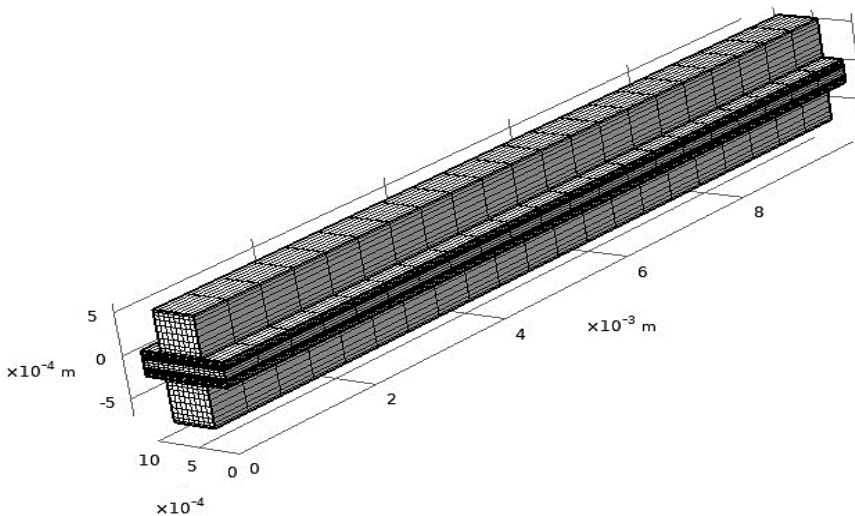


Figure 4. Mesh of the solid oxide fuel cell

3. Results and Discussion

The results of the study were achieved by considering the flow pattern co-current and counter current inside the cell. When the flow pattern was co-current, both the cathode and anode currents enter from the back of the fuel cell and exit from the front part of the cell. For counter current flow pattern, the inlet of the cathode flow channel is at the back of the cell while the inlet of the anode flow channel is in front of the fuel cell.

The graph in Figure 5 shows the average power density versus current density for both co-current and counter current flow patterns. As it is obvious from the plots, the potential of the cell decreases as the current density increases and the power density enhances at lower current densities, but it decreases when the current density passes a certain amount (about 1500 A.m⁻²). In addition, it can be seen that around the current density of 1500 A.m⁻², the two curves are slightly separated from each other, and this point also indicates the maximum power

density for the two current patterns. The value of the maximum power density for the co-current and counter current flow pattern was obtained as 1073 W.m^{-2} and 1050 W.m^{-2} , respectively.

Figure 6 also shows the trend of cell voltage changes versus current density. There is little difference between the voltages in the two current patterns. However, from the two graphs related to Figures 5 and 6, it is clear that the co-current flow has a more suitable performance in terms of power density and voltage.

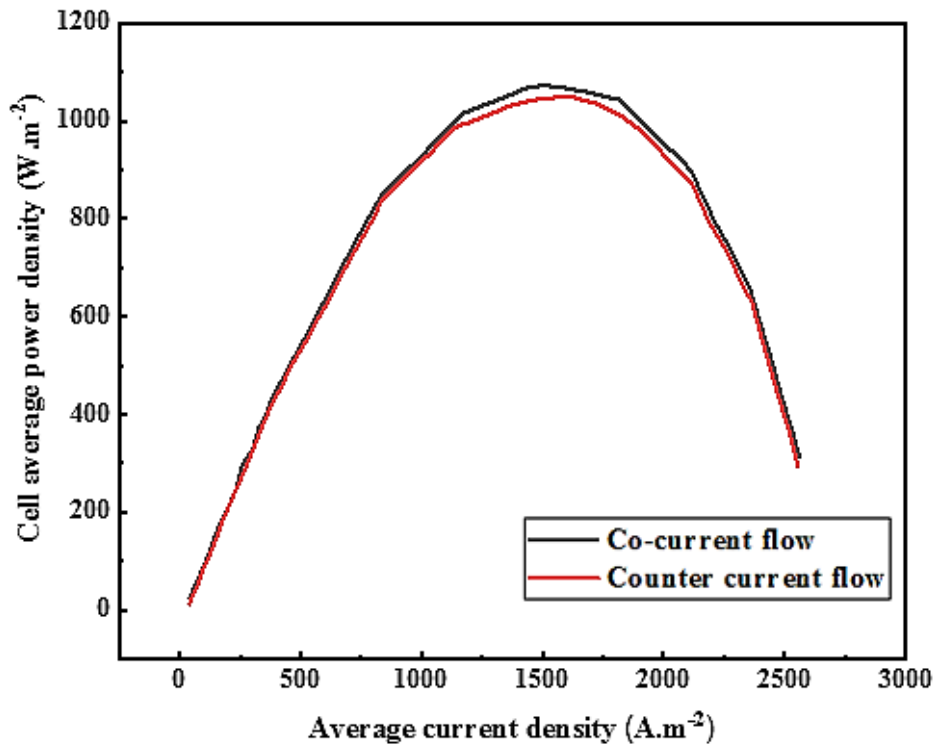


Figure 5. Power density- current density plot for co-current and counter-current flow pattern

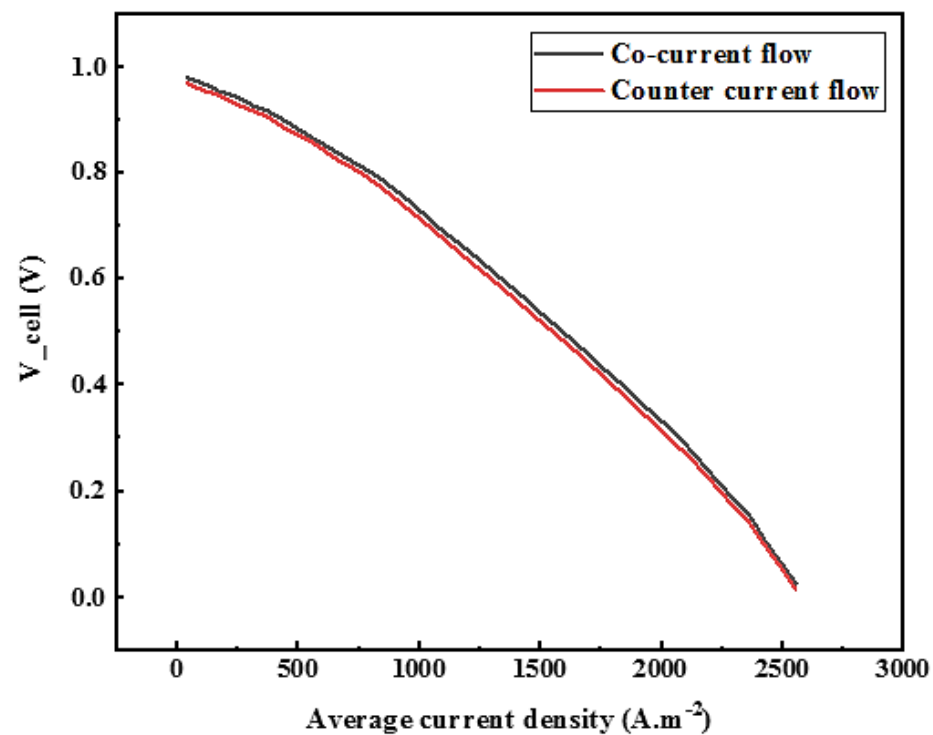


Figure 6. Cell voltage- current density plot for co-current and counter-current flow pattern

The distribution of the temperature, current, and concentration of chemical species are demonstrated in Figure 7 to Figure 14. Distributions of these parameters are connected to each other. In other words, when the concentration of hydrogen and oxygen is high, the reactions inside the cell occur faster and better and this way the produced heat and electrical current enhance and when the concentration of chemical species decreases the amount of generated heat and electricity reduce.

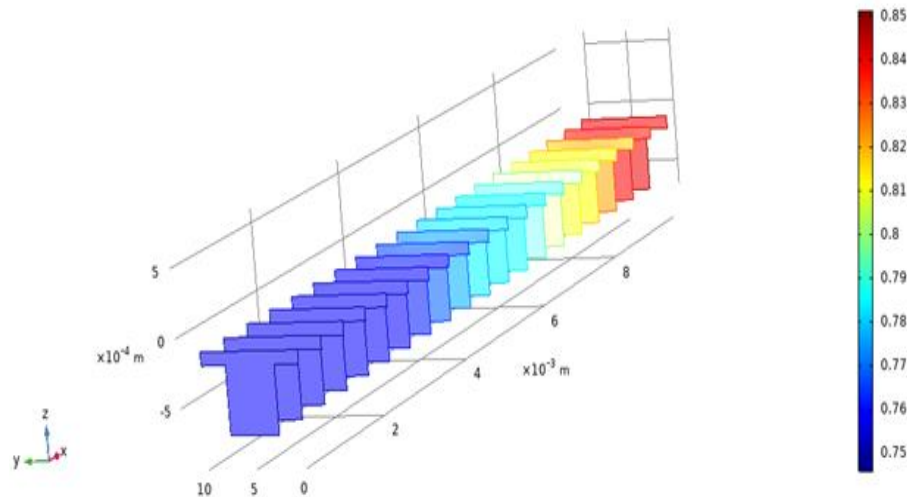


Figure 7. Distribution of molar fraction of H₂ inside the cell for co-current flow pattern

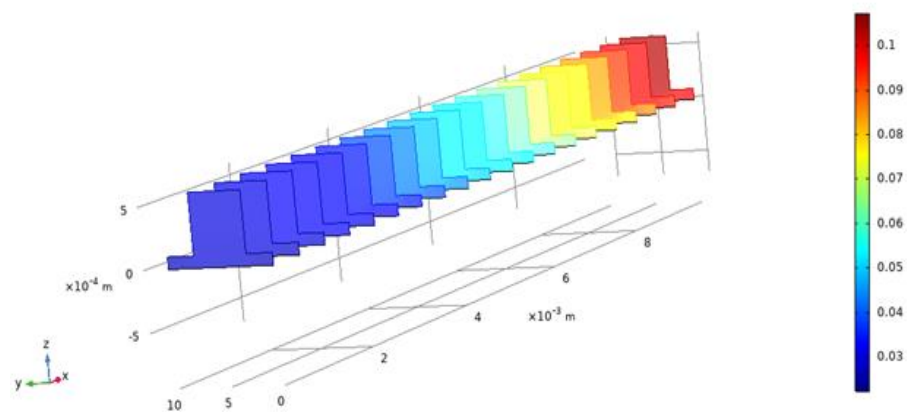


Figure 8. Distribution of molar fraction of O₂ inside the cell for co-current flow pattern

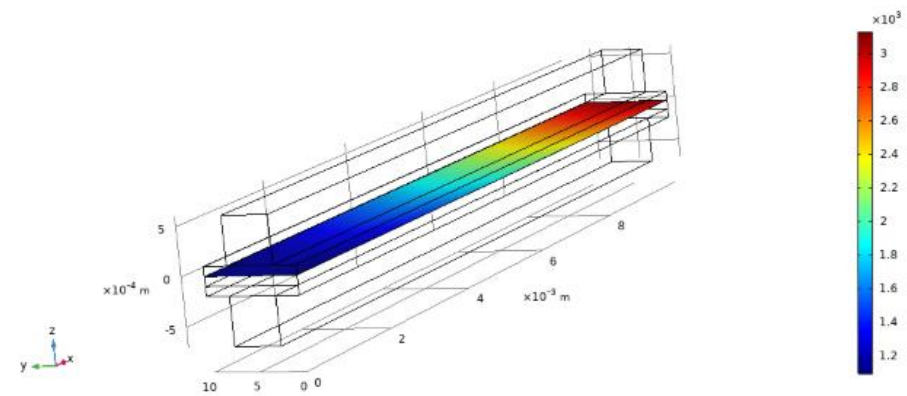


Figure 9. Distribution of current inside the cell for co-current flow pattern

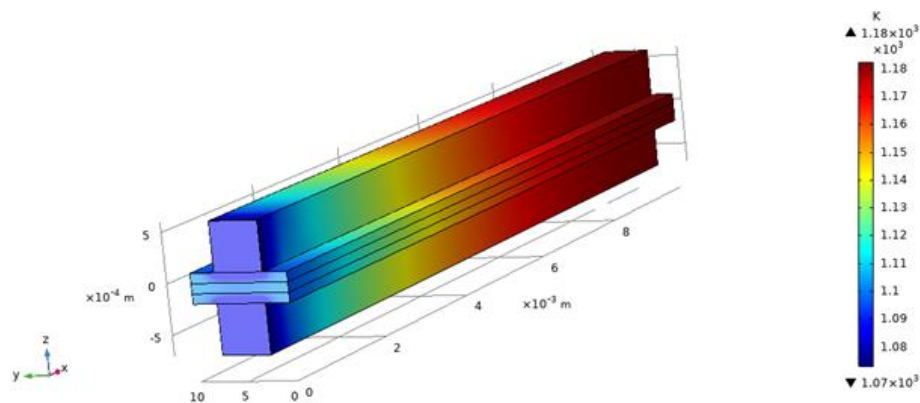


Figure 10. Distribution of temperature inside the cell for co-current flow pattern

For co-current flow pattern, the "3D temperature distribution" diagram (Figure 10) provides a 3D view of the temperature distribution throughout the fuel cell. According to this Figure 10, the maximum temperature is at the inlet of the fuel channel (anode side) and close to it. By analyzing the figure of the "molar hydrogen fraction (Figure 7)" at the inlet of the fuel channel, it is understood that the molar hydrogen fraction is also maximum and in the continuation of the channel with the reaction of hydrogen, its concentration decreases and reaction in anode side occurs and electricity is produced. In fact, at the beginning of the channel, where the hydrogen concentration is high, the electrochemical reaction of the fuel cell also takes place optimally, and at the end of the channel, this reaction and the hydrogen concentration are minimized. In general, the heat released by the half-cell reaction of the cathode is greater than the heat released by the half-cell reaction of the anode. That is, the electrochemical reaction of the fuel cell is exothermic (Mohammad Ebrahimi, 2017). Therefore, as can be seen, at the entrance of the channels, where the concentration is high, the current and temperature are also high. The heat released along the Z axis is transmitted mainly through convection to the gas channels (air and fuel), and then this heat exits from the flow channel with gas flow. As a result, the temperature inside the cell decreases.

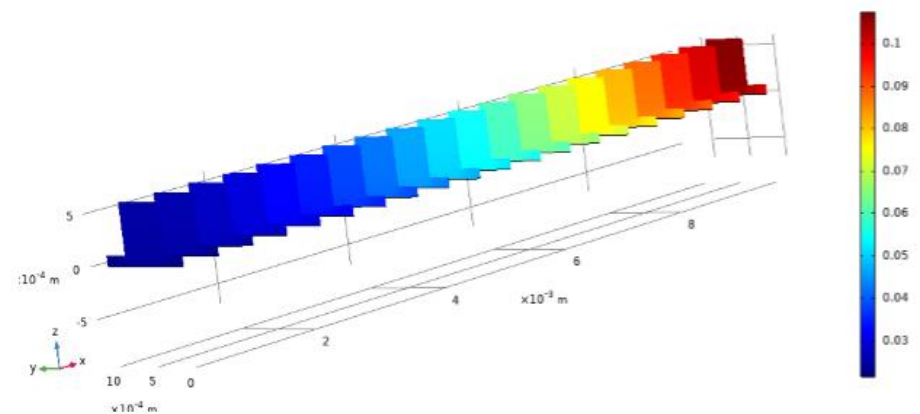


Figure 11. Distribution of molar fraction of O₂ inside the cell for counter-current flow pattern

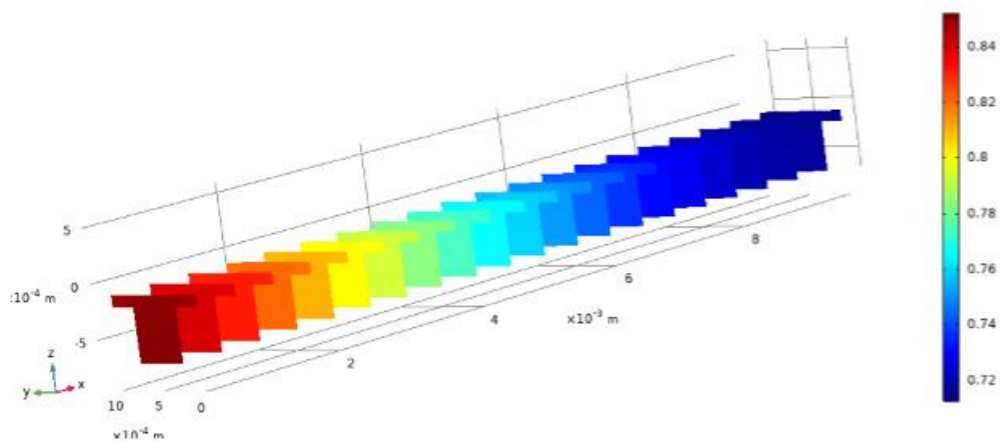


Figure 12. Distribution of molar fraction of H₂ inside the cell for counter-current flow pattern

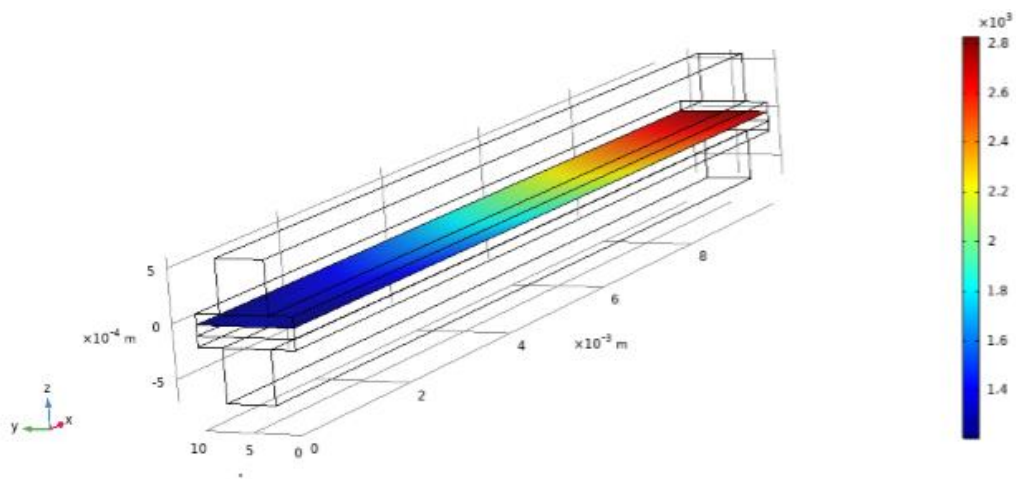


Figure 13. Distribution of current inside the cell for counter-current flow pattern

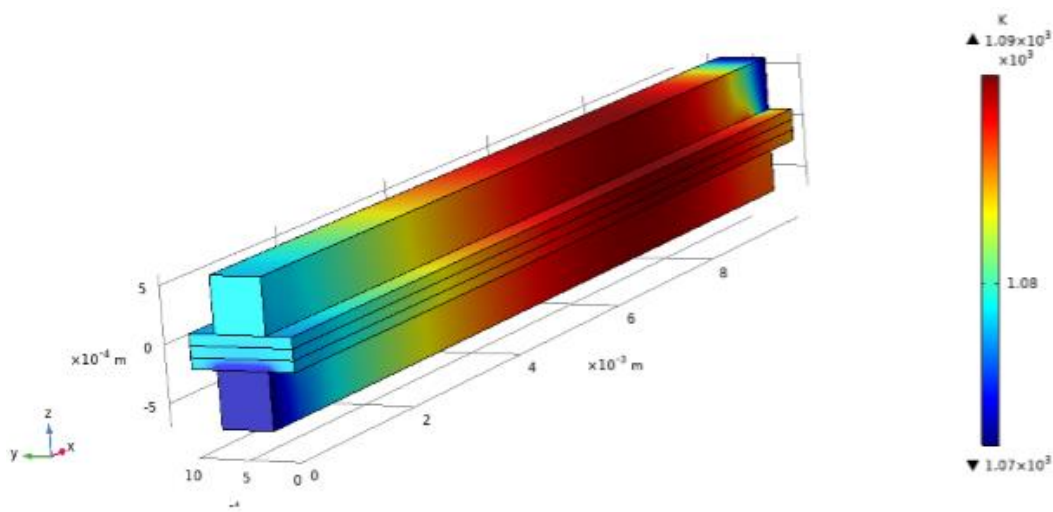


Figure 14. Distribution of temperature inside the cell for counter-current flow pattern

In counter-current flow pattern (Figure 11-14), the inlet gas of each channel from the other side of the fuel cell is in contact with the outlet of the other channel, so initially the temperature of the inlet gas to the channels drops. Then the temperature rises by performing the exothermic electrochemical reactions inside the cell. The temperature drops at the outlets of the channels again (Figure 14). Despite the fact that the concentration at the inlet is high (Figure 11, Figure 12), the temperature has its lowest value, and then even with the decrease in the concentration of the reaction material, followed by a decrease in the rate of reaction, the temperature increases and, also, the produced electricity enhances. That is because of the enhancement of the transforming of the chemical substances and reactions that occur in three-phase boundaries of the cell. According to the molar fraction diagrams, in the center of the cell, the maximum concentrations of both reactants (oxygen and hydrogen) are present at the reaction site. Only in the center of the fuel cell, the concentrations of these two substances are in the right amount to perform good reactions. Therefore, the electrochemical reactions in the center of the fuel cell are performed optimally, and the temperature in this area is high.

4. Conclusion

In this study, a 3D mathematical model of a SOFC is rendered which can demonstrate the temperature, concentration and current distributions inside the cell and the performance of the solid oxide fuel cell. In addition, the design parameter (flow pattern) of the inlet and outlet currents' influence on the performance of the cell was evaluated. In other words, the performance of the cell is calculated when the flow pattern changes from counter-current to co-current. The results stated that the distribution of temperature, current and concentration of reactants (O_2 and H_2) are related and wherever the concentration of materials is higher, the performance of the cell and the amount of the temperature and produced current enhance. Furthermore, changing the flow pattern from counter-current to co-current does not affect the efficiency of the cell significantly. However, the performance of the solid oxide fuel cell is better when the flow pattern is co-current.

Acknowledgements

The researchers extend their thanks and appreciation to the collaboration and support of the University of Tabriz, the Department of Physics at the University of Sakarya and the Scientific and Technological Research Council of Turkey (TUBITAK).

Author Contributions

S.Mehdi Rezvan: Simulate the mathematical modelling prepared by M.Ahangari.

Mohammad Ahangari: Prepared the requirements for mathematical modelling (parameters, equations, etc.)

Nagihan Delibas: Contributed to the formation of idea and provided scientific and financial support.

Soudabeh Bahrami: Prepared theoretical information about SOFCs and mathematical modelling.

Asgar Moradi: Contributed to debugging the computational works.

Aligholi Niaei: Contributed to the formation of idea and provided scientific and financial support.

Conflicts of Interest

The authors declared no potential conflicts of interest with respect to the research, authorship and publication of this article.

References

- Abdalla, A. M., Hossain, S., Azad, A. T., Petra, P. M. I., Begum, F., Eriksson, S. G., & Azad, A. K. (2018). Nanomaterials for solid oxide fuel cells: A review. *Renewable and sustainable energy reviews*, 82, 353-368. DOI: <https://doi.org/10.1016/j.rser.2017.09.046>
- Ahmad, M. Z., Ahmad, S. H., Chen, R. S., Ismail, A. F., Hazan, R., & Baharuddin, N. A. (2021). Review on recent advancement in cathode material for lower and intermediate temperature solid oxide fuel cells application. *International Journal of Hydrogen Energy*. DOI: <https://doi.org/10.1016/j.ijhydene.2021.10.094>

- Akkaya, A. V. (2007). Electrochemical model for performance analysis of a tubular SOFC. *International Journal of Energy Research*, 31(1), 79-98. DOI: <https://doi.org/10.1002/er.1238>
- Aydin, Ö., Matsumoto, G., & Shiratori, Y. (2021). Thermal stresses in SOFC stacks: the role of mismatch among thermal conductivity of adjacent components. *Turkish Journal of Chemistry*, 45(3), 719-736. DOI: <https://doi.org/10.3906/kim-2011-48>
- Aygün, B., Sariboğa, V., & Öksüzömer, M. A. F. (2021). Effect of fuel choice on conductivity and morphological properties of samarium doped ceria electrolytes for IT-SOFC. *Turkish Journal of Chemistry*, 45(5), 1408-1421. DOI: <https://doi.org/10.3906/kim-2104-56>
- Burnwal, S. K., Bharadwaj, S., & Kistaiah, P. (2016). Review on MIEC cathode materials for solid oxide fuel cells. *Journal of Molecular and Engineering Materials*, 4(02), 1630001. DOI: <https://doi.org/10.1142/S2251237316300011>
- Caliandro, P., Diethelm, S., & Nakajo, A. (2015). Electrochemical model of a triode solid oxide fuel cell. *ECS Transactions*, 68(1), 2387. DOI: <https://doi.org/10.1149/06801.2387ecst>
- Chiu, H.-C., Jang, J.-H., Yan, W.-M., Li, H.-Y., & Liao, C.-C. (2012). A three-dimensional modeling of transport phenomena of proton exchange membrane fuel cells with various flow fields. *Applied energy*, 96, 359-370. DOI: <https://doi.org/10.1016/j.apenergy.2012.02.060>
- Delibaş, N., Gharamaleki, S. B., Mansouri, M., & Niaei, A., Reduction of operation temperature in SOFCs utilizing perovskites. *International Advanced Researches and Engineering Journal*, 6(1), 56-67. DOI: <https://doi.org/10.35860/iarej.972864>
- Ferriday, T. B., & Middleton, P. H. (2021). Alkaline fuel cell technology-A review. *International Journal of Hydrogen Energy*, 46(35), 18489-18510. DOI: <https://doi.org/10.1016/j.ijhydene.2021.02.203>
- Grondin, D., Deseure, J., Ozil, P., Chabriat, J.-P., Grondin-Perez, B., & Brisse, A. (2013). Solid oxide electrolysis cell 3d simulation using artificial neural network for cathodic process description. *Chemical Engineering Research and Design*, 91(1), 134-140. DOI: <https://doi.org/10.1016/j.cherd.2012.06.003>
- Hussain, S., & Yangping, L. (2020). Review of solid oxide fuel cell materials: Cathode, anode, and electrolyte. *Energy Transitions*, 4(2), 113-126. DOI: <https://doi.org/10.1007/s41825-020-00029-8>
- Ilbas, M., & Kumuk, B. (2019). Numerical modelling of a cathode-supported solid oxide fuel cell (SOFC) in comparison with an electrolyte-supported model. *Journal of the Energy Institute*, 92(3), 682-692. DOI: <https://doi.org/10.1016/j.joei.2018.03.004>
- Kakac, S., Pramuanjaroenkij, A., & Zhou, X. Y. (2007). A review of numerical modeling of solid oxide fuel cells. *International Journal of Hydrogen Energy*, 32(7), 761-786. DOI: <https://doi.org/10.1016/j.ijhydene.2006.11.028>
- Kurahashi, N., Murase, K., & Santander, M. (2022). High-Energy Extragalactic Neutrino Astrophysics. *arXiv preprint arXiv:2203.11936*. DOI: <https://doi.org/10.48550/arXiv.2203.11936>
- Laosiripojana, N., Wiyaratn, W., Kiatkittipong, W., Arpornwichanop, A., Soottitantawat, A., & Assabumrungrat, S. (2009). Reviews on solid oxide fuel cell technology. *Engineering Journal*, 13(1), 65-84. DOI: <https://doi.org/10.4186/ej.2009.13.1.65>
- Li, P.-W., & Suzuki, K. (2004). Numerical modeling and performance study of a tubular SOFC. *Journal of the Electrochemical Society*, 151(4), A548. DOI: <https://doi.org/10.1149/1.1647569>
- Mohammad Ebrahimi, I. (2017). Three-dimensional modeling of transport phenomena in a planar anode-supported solid oxide fuel cell. *Iranian Journal of Hydrogen & Fuel Cell*, 4(1), 37-52. DOI: <http://doi.org/10.22104/IJHFC.2017.2342.1144>
- Ranasinghe, S. N., & Middleton, P. H. (2017). *Modelling of single cell solid oxide fuel cells using COMSOL multiphysics*. Paper presented at the 2017 IEEE International Conference on Environment and Electrical Engineering and 2017 IEEE Industrial and Commercial Power Systems Europe (EEEIC/I&CPS Europe). DOI: <https://doi.org/10.1109/EEEIC.2017.7977790>
- Shaari, N., Kamarudin, S. K., Bahru, R., Osman, S. H., & Md Ishak, N. A. I. (2021). Progress and challenges: Review for direct liquid fuel cell. *International Journal of Energy Research*, 45(5), 6644-6688. DOI: <https://doi.org/10.1002/er.1238>
- Shu, L., Sunarso, J., Hashim, S. S., Mao, J., Zhou, W., & Liang, F. (2019). Advanced perovskite anodes for solid oxide fuel cells: A review. *International Journal of Hydrogen Energy*, 44(59), 31275-31304. DOI: <https://doi.org/10.1016/j.ijhydene.2019.09.220>
- Singh, M., Zappa, D., & Comini, E. (2021). Solid oxide fuel cell: Decade of progress, future perspectives and challenges. *International Journal of Hydrogen Energy*, 46(54), 27643-27674. DOI: <https://doi.org/10.1016/j.ijhydene.2021.06.020>

- Stambouli, A. B., & Traversa, E. (2002). Solid oxide fuel cells (SOFCs): a review of an environmentally clean and efficient source of energy. *Renewable and sustainable energy reviews*, 6(5), 433-455. DOI: [https://doi.org/10.1016/S1364-0321\(02\)00014-X](https://doi.org/10.1016/S1364-0321(02)00014-X)
- Suzuki, M., Shikazono, N., Fukagata, K., & Kasagi, N. (2008). Numerical analysis of coupled transport and reaction phenomena in an anode-supported flat-tube solid oxide fuel cell. *Journal of power sources*, 180(1), 29-40. DOI: <https://doi.org/10.1016/j.jpowsour.2008.02.039>
- Tseronis, K., Bonis, I., Kookos, I., & Theodoropoulos, C. (2012). Parametric and transient analysis of non-isothermal, planar solid oxide fuel cells. *International Journal of Hydrogen Energy*, 37(1), 530-547. DOI: <https://doi.org/10.1016/j.ijhydene.2011.09.062>
- Tseronis, K., Bonis, I., Kookos, I., & Theodoropoulos, C. (2012). Parametric and transient analysis of non-isothermal, planar solid oxide fuel cells. *International Journal of Hydrogen Energy*, 37(1), 530-547. DOI: <https://doi.org/10.1016/j.ijhydene.2011.09.062>
- Wang, G., Yang, Y., Zhang, H., & Xia, W. (2007). 3-D model of thermo-fluid and electrochemical for planar SOFC. *Journal of power sources*, 167(2), 398-405. DOI: <https://doi.org/10.1016/j.jpowsour.2007.02.019>
- Xia, C., Rauch, W., Wellborn, W., & Liu, M. (2002). Functionally graded cathodes for honeycomb solid oxide fuel cells. *Electrochemical and solid-state letters*, 5(10), A217. DOI: <https://doi.org/10.1149/1.1503203>
- Yakabe, H., Ogiwara, T., Hishinuma, M., & Yasuda, I. (2001). 3-D model calculation for planar SOFC. *Journal of power sources*, 102(1-2), 144-154. DOI: [https://doi.org/10.1016/S0378-7753\(01\)00792-3](https://doi.org/10.1016/S0378-7753(01)00792-3)
- Yaoxuan, Q., Cheng, F., & Kening, S. (2021). *Multiphysics simulation of a solid oxide fuel cell based on COMSOL method*. Paper presented at the E3S Web of Conferences. DOI: <https://doi.org/10.1051/e3sconf/202124501005>